Multipropeller Whirl Flutter Stability Study using Multibody Dynamics Analysis with Component Mode Synthesis Element

Kyle J. Nelson[1], Jinwei Shen[1], Andrew R. Kreshock[2], Carol Wieseman[3], and Josiah M. Waite[3]
[1]*The University of Alabama , Tuscaloosa, Alabama 35401*
[2]*U.S. Army Combat Capabilities Development Command Army Research Laboratory , Hampton, Virginia 23666*
[3]*NASA Langley Research Center, Hampton, VA, 23681*

I. Introduction

Increasing demand for alternative forms of energy is bringing exciting developments to transportation. The NASA X-57 Maxwell, a new X-Plane project (Fig. 1a), is a fully electric vehicle that is bringing some new technologies to increase the efficiency of the plane and lower emissions [1]. Based on the Italian built Tecnam P2006T, the X-57 Maxwell is the latest iteration of The Scalable Convergent Electric Propulsion Technology and Operations Research (SCEPTOR). Using electric propulsion, as well as other design considerations, the X-57 aims to be significantly more efficient in cruising flight compared to the Tecnam P2006T [2, 3].

The X-57 features 14 propellers installed along the wing, all driven by electric motors (Fig. 1b and Table 2). Two large propellers installed on the wing tips, named tip propellers or cruise propellers, are the main propulsive devices, operating throughout flight. The other twelve smaller propellers installed inboard along the wing and upstream of the wing leading-edge, named high-lift propellers, are designed to be operative during takeoff and landing phases of the flight, and meant to augment wing lift at low speeds. These high-lift propellers are mounted using spring-loaded, folding hinges near the root of each propeller that cause them to fold against the nacelle while not in operation (i.e., during cruise). These high-lift propellers were based on studies during NASA's LEAPTech experiment [4, 5].

(a) NASA X-57 Maxwell Illustration

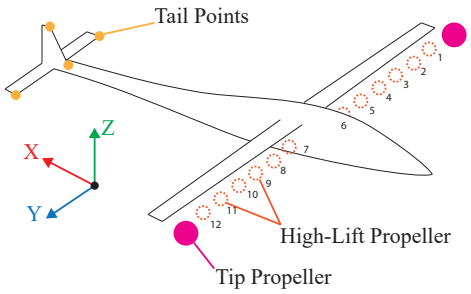

(b) X-57 Modal-Super-Element (MSE) Model

Fig. 1 NASA X-57 Maxwell, an Electric Propeller Aircraft, and its MSE Model

As it is required by FAA regulations for any new civil aircraft development, aeroelastic stability evaluations need to be performed to insure vehicle does not encounter any critical instability scenarios. Propeller whirl flutter, where propeller aerodynamics drive the coupled motion of the airframe and pylon to become unstable at high forward speeds, is one potential instability for the X-57. Taylor and Browne discovered propeller whirl flutter analytically in 1938, but it was not a design consideration of the aircraft of the era due to the speed limitations of the available aircraft [6]. Unfortunately, two fatal crashes of Lockheed Electra aircraft in the early 1960s brought the topic of propeller whirl flutter back into design consideration after it was determined to be the cause of the crashes. NASA Transonic Dynamics Tunnel (TDT) was used for scale model recreations of the crashes [7] . And it was determined that a damaged pylon mount weakened the structure such that whirl flutter was able to occur [8]. Since then, more studies on propeller flutter have been performed [9]. In particular, tiltrotor whirl flutter has drawn a lot of interest [10–12].

The X-57 features a new higher aspect ratio wing designed to help achieve an increase in cruise efficiency. This new wing has roughly 45% of the wing area of the Tecnam. Such a change in wing dimensions, the relocation of the

[‡]Courtesy of NASA

main drive propellers to the wing tip, and the addition of the 12 inboard high-lift propellers, have raised concerns for propeller whirl flutter. Table 1 presents aircraft parameters. Table 2 presents propeller parameters.

Property	Value
Critical Takeoff Speed (kts)	58
Cruise Speed (kts)	150
Wing Semi-Span (ft)	14
Wing Nominal Chord (ft)	2.1
Aircraft Weight (lb)	3,000

Table 1 Key Aircraft Parameters

Property	Tip Propeller	High-Lift Propeller
Number of Rotors	2	12
Number of Blades	3	5
Diameter (ft)	5	1.9
Take-Off RPM	2700	Variable
Cruise RPM	2250	0
Airfoil	Composition	MH114

Table 2 Key Propeller Parameters

A major challenge to predicting propeller whirl flutter is the complex interaction of propeller aerodynamics and airframe/wing/pylon structural dynamics. Previously, the traditional method to determine the whirl-flutter boundary was with extensive wind-tunnel testing [10, 11, 13]. Development of computational modeling software, such as Multibody Dynamics codes, are fast becoming the alternative methods for analyzing complex aeroelastic phenomena. The rotorcraft community have used multibody dynamics heavily thanks to its generality and ability to model complex rotorcraft and propeller aeromechanical systems [12, 14]. Two such multibody dynamics codes are Dymore and CAMRAD, which are used in this study to predict the whirl-flutter boundary of X-57.

A challenge in multibody dynamics simulation of X-57 propeller whirl flutter is how to model the complex structural dynamics of the airframe/wing/propeller pylon structures. Although a detailed NASTRAN model has been developed for the X-57 airframe and wing, such a model cannot be directly integrated into multibody dynamics simulations due to its complexity and large size. Component mode sythesis approaches, such as Herting reduction, can provide smaller representations of large complex mechanical systems [15, 16], and the reduced order model can be integrated in Dymore as a modal-super-element [17]. Such techniques are based on the projection of the original equations of motion onto a subspace of the configuration space and provide reduced equations that represent the dynamic behavior of the original system accurately within a desired frequency range. Detailed information about the original component can be obtained by expanding the solution of the reduced system in a recovery step. The fuselage, landing gear, tail, and main wing are captured with a reduced order model derived from a NASTRAN FEM model using component mode synthesis approach (Fig. 1b).

The objectives of this paper are to

1) explore the use of component mode synthesis elements to predict multipropeller whirl flutter,
2) investigate the contributions of multiple inboard propellers on whirl-flutter stability, in particular, the effects of these propeller's wing-span locations.

II. Analytical Models

Dymore is a finite element (FE) based multibody dynamics code for the comprehensive modeling of nonlinear flexible multibody systems [18]. Derived in an inertial Cartesian frame, the equations of motion and constraints are

set up using the Lagrange multiplier method. This approach forms a set of differential-algebraic equations that are then solved using a robust time integration scheme. The element library in Dymore includes rigid and deformable bodies as well as joint elements. The deformable bodies are set up using the FE method with the beams and shells modeled as geometrically exact. In addition, deformable bodies can be modeled with a modal-super-element, reduced order structure model generated with the component mode synthesis approach. The aerodynamic forces in Dymore are computed either by using a built-in lifting line theory or through external aerodynamic code coupling. Dymore predicts whirl-flutter stability by numerically perturbing the model, and extracting damping with the transient response (details at Section. II.C).

CAMRAD is an aeromechanical analysis for helicopters and rotorcraft that incorporates several tools, including multibody dynamics, nonlinear FE, structural dynamics, and rotorcraft aerodynamics [19]. CAMRAD is the chosen tool of NASA engineers and the primary code to which the results from Dymore are compared. The aeroelastic stability of the dynamic system, i.e. whirl-flutter stability in this study, is determined through direct eigen-analysis of the linearized equations of motion.

A. Dymore Modal-Super-Element Model of X-57 Airframe/Wing/Pylon

Previous Dymore models of the X-57 used equivalent beam models to represent the semispan and full-span wings [20]. The flexibility of the fuselage was captured with limited success through tuned springs and optimized equivalent beams. This ad hoc modeling of X-57 airframe/wing/pylon structure is time-consuming and less accurate due to the limitation of beam and spring elements. The current Dymore model uses a modal-super-element obtained through Herting reduction of the full NASTRAN X-57 model. This component mode synthesis approach is more accurate and time-saving as the Herting reduction can be computed routinely while the X-57 NASTRAN model evolves with design progress. This advancement removes the need for optimization of equivalent beams and tuned springs to capture the dynamics of the complex X-57 airframe/wing/pylon structures. In the Herting reduction process, interface nodes are retained as (*a*) hub locations for the 14 propellers fitted to the X-57, (*b*) two points on the fuselage to constrain the model, and (*c*) points to include the displacements of the tail (Fig. 1b). Table 3 shows the comparison of the reduced order model frequencies with those of the full NASTRAN free-free X-57 model. Agreement between the reduced order model and the full NASTRAN FEM is good.

Table 3 Comparison of Frequencies of Herting Reduction Model to the NASTRAN X-57 Free-Free Model

MODE	NASTRAN	Herting Reduction	Description
7	3.04	3.05	1st Sym. Out-of-Plane
8	5.67	5.72	1st ASym. Out-of-Plane
9	6.97	7.06	1st ASym. Inplane
10	9.92	10.01	1st Sym. Inplane
11	11.44	11.50	2nd Asym. Out-of-Plane
12	12.05	12.37	2nd Sym. Out-of-Plane
13	13.70	13.96	1st Sym. Torsion
14	14.16	14.45	1st Asym. Torsion
15	15.61	16.06	1st Asym. Empanage w/Torsion

B. Dymore Modeling of Propeller Systems

The high-lift propeller shown in Fig. 2a is a fixed-pitch propeller and has the folding hinge near the blade root to allow the blades to fold. The folding hinge orientation is designed to allow the propeller blades to fold and conform to the nacelle when not in operation to reduce drag. The folding hinge is located at 23% of the blade radius. The tip propeller model shown in Fig. 2b consists of an elastic blade with a variable pitch. All propellers included in this model have a driven revolute joint that can be set to the desired RPM for the flight condition.

The propeller aerodynamics are calculated with a lifting line approach based on airfoil look-up tables combined with a uniform inflow model [21]. The airfoil look-up tables are generated with a 2D CFD code.

[‡]Courtesy of NASA

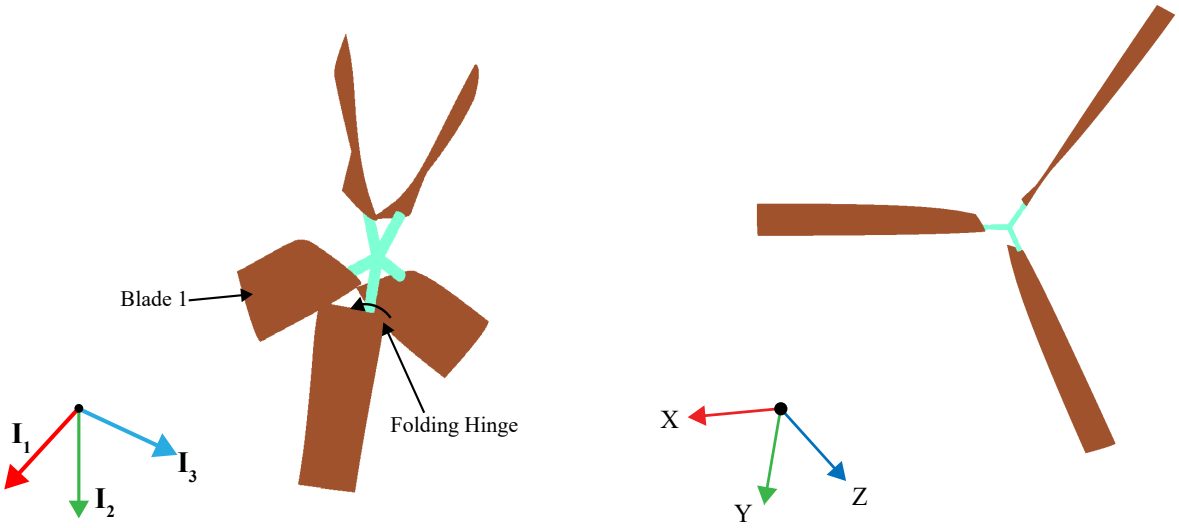

(a) Dymore Model of High Lift Propeller **(b) Dymore Model of Tip Propeller**

Fig. 2 Dymore Models of X-57 Propellers

C. Dymore Approach in Predicting Whirl Flutter

The whirl-flutter stability of the full-span X-57 aircraft is calculated from both wing tip motions after perturbations are applied on the two wing tips. The in-phase perturbations are used to excite symmetric wing modes whereas out of phase perturbations are used for antisymmetric wing modes. The wing modes are perturbed at each mode's natural frequency and the transient responses of the two wing tips are recorded. Dymore uses the Prony method to identify the wing mode frequency and damping based on the transient responses [21, 22].

D. CAMRAD Model Used in Predicting Whirl Flutter

CAMRAD has several builtin rotor aerodynamics models such as different unsteady aerodynamics models and inflow models [19]. The current CAMRAD model uses a similar approach for the propeller aerodynamics as the Dymore model. The structural model of the X-57 fixed system, which include wing, fuselage, and empennage, uses the modal displacements at the propeller hub locations. This modal representation of the X-57 fixed-system is obtained from linear eigenvalue analysis of the full X-57 NASTRAN model.

III. Analytical Results

This section presents the whirl-flutter results from: (*a*) a parametric study of a high-lift propeller wing spanwise location on whirl-flutter stability, and (*b*) whirl-flutter stability of all 14 propellers operating under various flight conditions. The parametric study of high-lift propeller spanwise location is carried out only with Dymore analysis. The whirl-flutter stability of all 14 propellers is compared between Dymore and CAMRAD predictions. There is no structural damping included in either the wing or the rotor system of the analytical models. In addition, the wing aerodynamics are not modeled as they typically influence whirl-flutter stability by simply adding to the damping from the propeller aerodynamics. The source of wing damping is thus purely the propeller aerodynamics.

A. Parametric Study of the Effect of High-Lift Propeller Wing-Span Location on Whirl Flutter

The high-lift propellers mounted to the X-57 are used only during the takeoff and landing phases of flight. At such low speeds, the individual propellers are not expected to be at a risk for the onset of propeller whirl flutter. However, it is of interest to study the effect of propeller wing-span location on whirl-flutter stability. Examining the influence of the location of a single pair of high-lift propellers on the whirl-flutter modes helps to understand their contributions to those of the full 14-propeller system. The parametric study is carried out to have a single pair of high-lift propellers operating at a time with the others not spinning. The pairs are formed by the propellers mirroring to each other across wing-span. Moving from wing tip to wing root, the pairs of propellers are: Nacelle 1 and 12, 2 and 11, 3 and 10, 4 and 9, 5 and 8,

and lastly Nacelle 6 and 7 (Fig˙ 1b). There is no structural damping assumed either in the wing or the propellers. This parametric study considers the high-lift propellers operating at a fixed 4400 RPM. The flight speed range is extended beyond the designed high-lift propeller operation range. Only Dymore analysis is used in this parametric study.

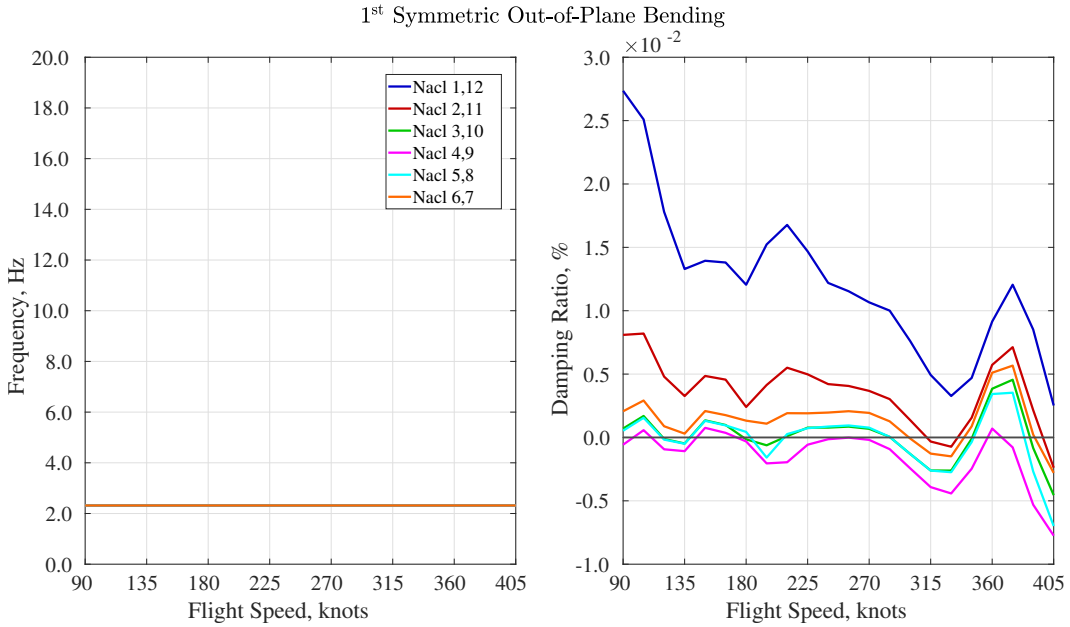

Fig. 3 High-Lift Propeller Location Influence on Symmetric Wing Out-of-Plane Bending Mode.

Figures 3 to 7 illustrate the effect of high-lift propeller spanwise location on the frequencies and damping ratios of the first five wing modes. As the high-lift propellers are relatively small compared to the typical thrust-generating counterparts, such as the tip propellers, their inertial and aerodynamic influence on the wing modes is small. These figures overall show the location of the high-lift propeller has a negligible effect on the wing frequencies. The wing damping ratio magnitude is shown to be small, but its variation with propeller location is examined below.

Figure 3 shows the effect of the location of pairs of high-lift propellers along the wing span on the symmetric wing out-of-plane bending mode. An interesting observation is made that the pair of rotors with the least influence is not located closest to the wing root. This pair of rotors (nacelle 4,9) are in the third position outboard from the cockpit and have a small, negative influence on symmetric out-of-plane bending.

Figure 4 presents the influence of the high-lift propeller position on the antisymmetric wing out-of-plane bending mode. Unlike the previous figure that had a distinct difference in damping based on the location of the propeller, this is not observed here. The damping of the high-lift propeller pairs is of the same small magnitude, but there is a uniform stable response from all locations along the wing span. This damping is also influenced by the thrust generated with increasing flight speed. The bottom of the 'bowl' shape made reflects the transition of positive to negative thrust.

Figure 5 presents the influence of high-lift propeller position on the antisymmetric wing inplane bending mode. Similar to the antisymmetric out-of-plane bending mode, there is great uniformity between all pairs of rotors. Unlike the previous result, the transition from positive to negative damping creates a steady negative trend to instability. The total influence on this mode shares the same small 0.01% damping that is observed in Figs. 3 and 4.

Figure 6 presents the influence of the high-lift propeller location on symmetric wing inplane bending mode. The outboard three propeller pairs have the highest damping ratio at low speeds but the damping ratio drops quickly with increasing flight speed. The high-lift rotor pair 3 and 10 have positive damping at low speeds but becomes negative from 135 knots and remain flat to the end of the speed range. A different trend is observed with the three in-board pairs of high-lift propellers. All three pairs have negative damping and very small deviation until 225 knots, but then produce positive damping with increasing flight speed.

Figure 7 presents the influence of the high-lift propeller location on the wing the symmetric torsional mode. The wing damping ratio magnitude from propeller aerodynamics is the greatest of all the five modes discussed. This is also the only mode that shows a decreasing amount of damping as the propellers are moved inboard from the wingtip. The stabilizing response of this mode comes from the rotors pitching in and out of the axial flow condition with blade

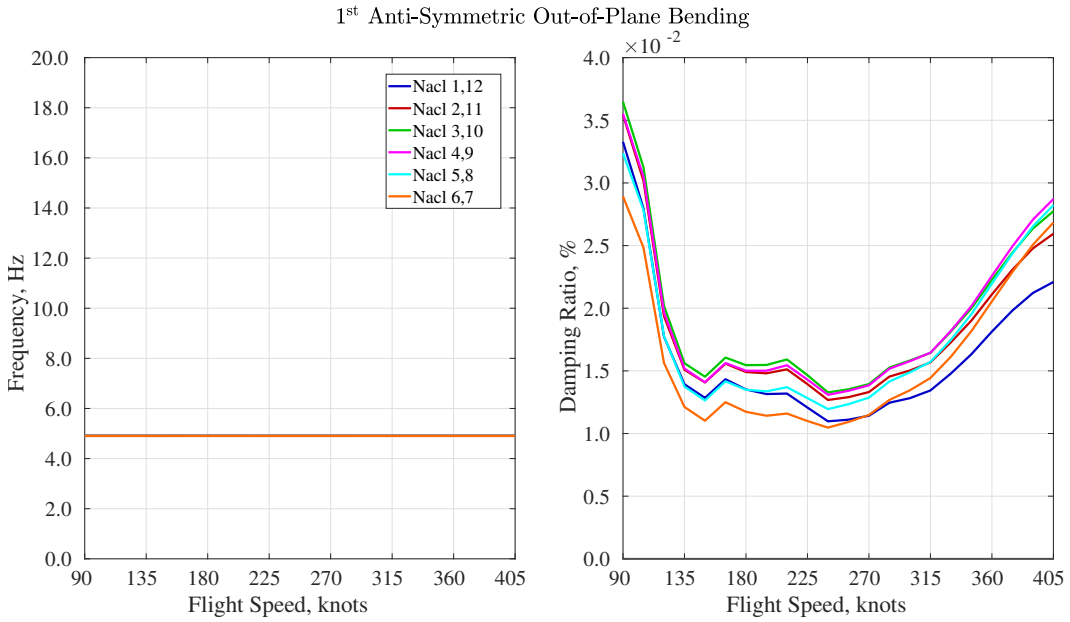

Fig. 4 High-Lift Propeller Location Influence on Antisymmetric Wing Out-of-Plane Bending Mode.

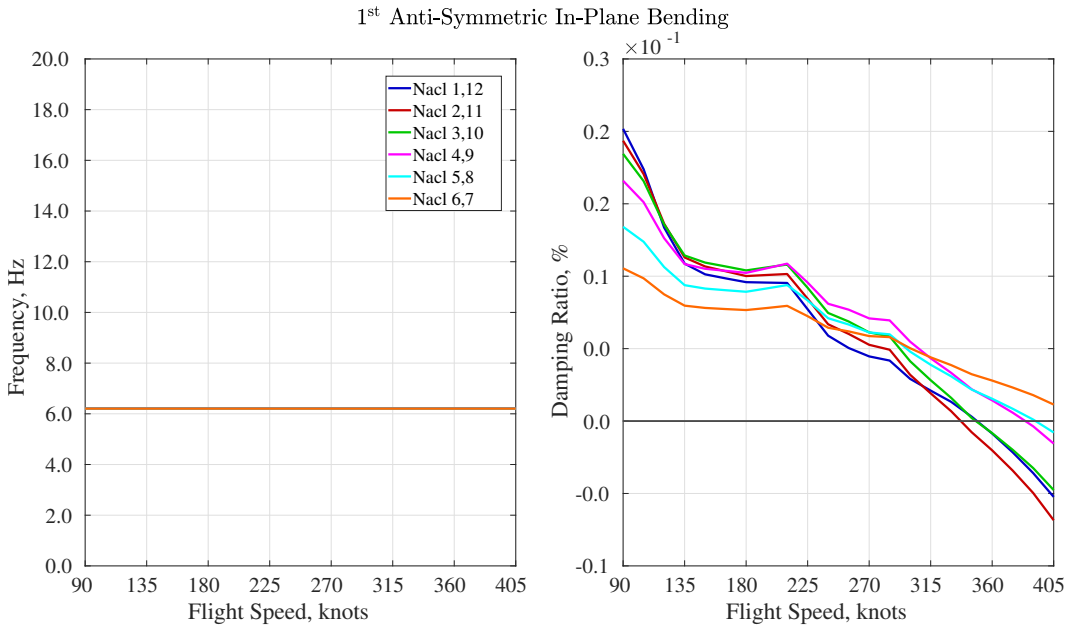

Fig. 5 High-Lift Propeller Location Influence on 1st Antisymmetric Wing Inplane Bending Mode.

flapping. Although the propeller blades are assumed rigid, the folding hinge allows the blades to flap.

B. Whirl Flutter Stability of X-57 Model with 14 Propellers

Comparison of whirl-flutter stability between Dymore and CAMRAD analyses of the X-57 with 14 propellers is detailed in this section. All comparisons simulate the aircraft at 8,000 ft with flight speeds ranging from 50–350 knots. The tip propellers are trimmed to 0 thrust measured at the rotor hub, with RPM 2700 for cruise flight. There are three RPM cases for the high-lift propellers: 0 RPM (simulating the folded condition), a scheduled RPM sequence with increasing speed (Table 4), and a 5940 overdrive RPM.

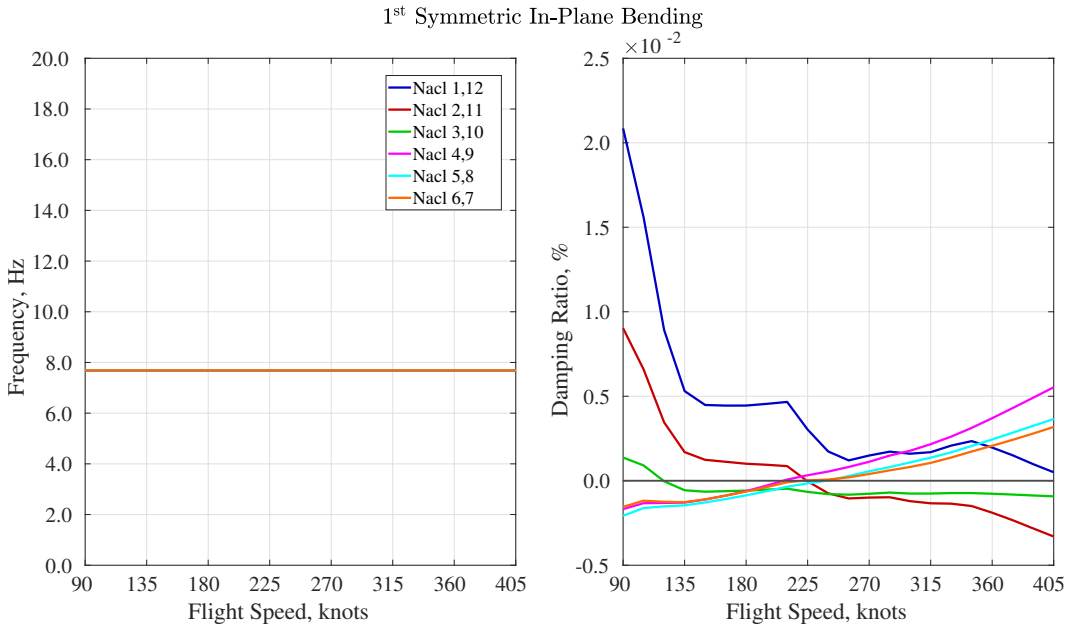

Fig. 6 High-Lift Propeller Location Influence on Symmetric Wing Inplane Bending Mode.

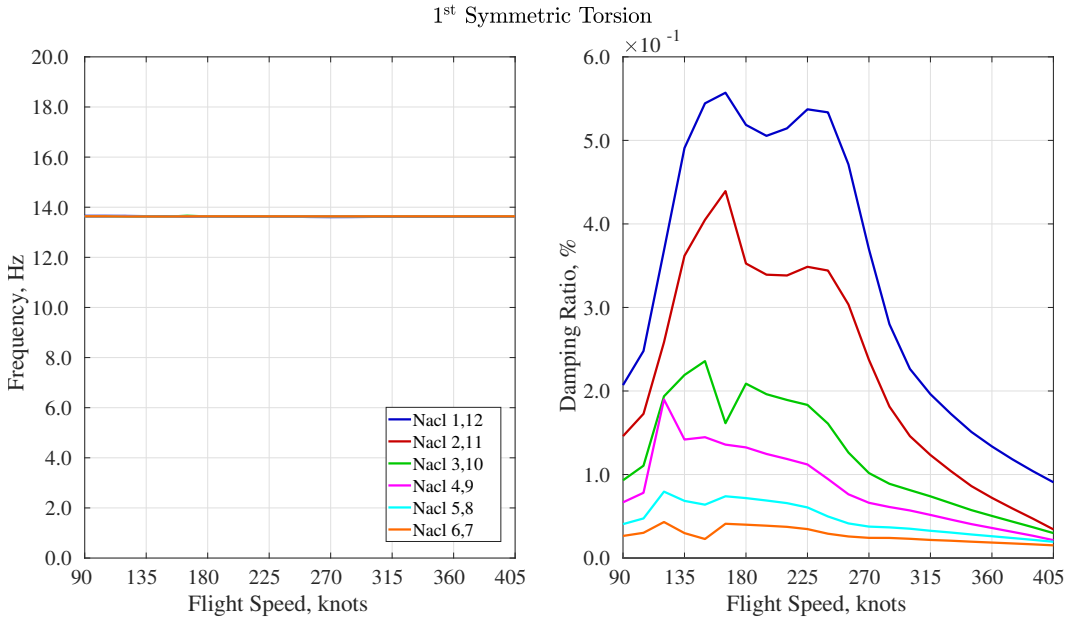

Fig. 7 High-Lift Propeller Location Influence on Symmetric Wing Torsional Bending Mode.

Table 4 High-Lift Propeller RPM Schedule for Increasing Flight Speed

Speed (KTAS)	50	60	70	80	90	100	110	120	>120
RPM	5314	5295	4848	4456	4118	4529	4959	5388	5388

Figure 8 shows the wing frequency and damping variation with flight speed with a high-lift propeller RPM remaining at 0 (simulating folded-away propellers). The comparison of frequencies between Dymore and CAMRAD is good for the first four modes. There are small disagreements in the modal frequencies for the symmetric and antisymmetric torsional modes. Dymore predictions of these modes are slightly higher than those of the CAMRAD, which is caused

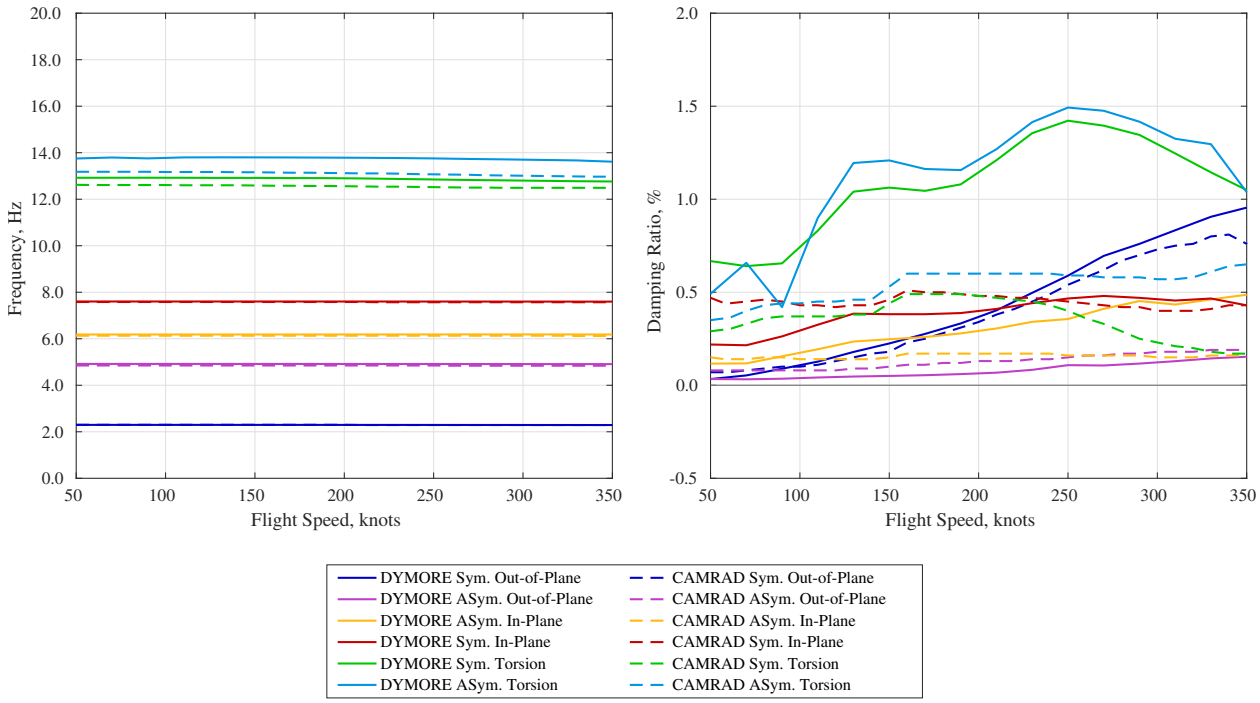

Fig. 8 Wing Frequency and Damping Ratio vs. Flight Speed, 0 High-Lift Propeller RPM.

by the small elevation of frequencies in these two modes after Herting reduction (Table 3). Overall, good agreements is shown in the predictions of damping ratios for all the modes except the symmetric and antisymmetric torsion modes. Different blade structure models in the two codes (Dymore blades are flexible beams while CAMRAD uses rigid blades) cause the discrepancies shown between the damping predictions of the torsion modes. The missing blade flexibility in the CAMRAD model leads to low damping for the wing torsion modes. The first symmetric out of plane bending mode damping is shown with an almost linear increase with flight speed which similar trends were observed with a previous study [23]. The damping of first wing antisymmetric out of plane modes and the two inplane modes are all low, showing a small increase or no change with the speed variation. Both Dymore and CAMRAD predict these modes to be stable throughout the speed range.

Figure 9 displays the wing frequency and damping variation with flight speed with a scheduled RPM condition for the high-lift propellers. The frequency and damping comparison between the two codes show similar trends as observed in the high-lift propeller folded case (Fig. 8). Dymore results show the operational high-lift propellers drive the first symmetric out of plane mode and the antisymmetric inplane slightly unstable at low speeds. This slight instability shown is of little concern for operational safety as the wing structural and aerodynamic damping, which is not included, is enough to raise these modes to stability. In addition, this instability becomes stable as speed increases beyond 75 knots. The inclusion of high-lift-propellers has a small influence on the other modes except for the two torsion modes. CAMRAD predictions show these modes remaining stable at low speed, though the damping ratio is low. The cause for this discrepancy is likely the difference in damping modeling approaches between the two codes (Dymore uses the Prony method to extract damping from transient wing response after artificial perturbation whereas CAMRAD calculates damping by performing eigenanalysis with the linearized equation of motion). The damping of the two torsion modes show more flattened variation with increasing speed, as compared to Fig. 8, and a small reduction of peak damping ratio at 250 knots.

Figure 10 presents the wing frequency and damping variation with flight speed and the overdrive high-lift propeller condition (5940 RPM). Over-driving the high-lift propellers eliminates the Dymore predicted low-speed negative damping observed in Fig. 9 for the 1st symmetric out of plane bending mode. Little change is observed by overdriving the high-lift propellers on the wing modes except that noted above. The damping ratio of wing mode variations with speed are similar to those of the scheduled propeller RPM cases (Fig. 9). Agreement between Dymore and CAMRAD is good for the damping ratio predictions of the symmetric out of plane and inplane modes. Agreement between the two codes is fair for the damping ratio predictions of the antisymmetric out of plane and inplane modes. Dymore predicted

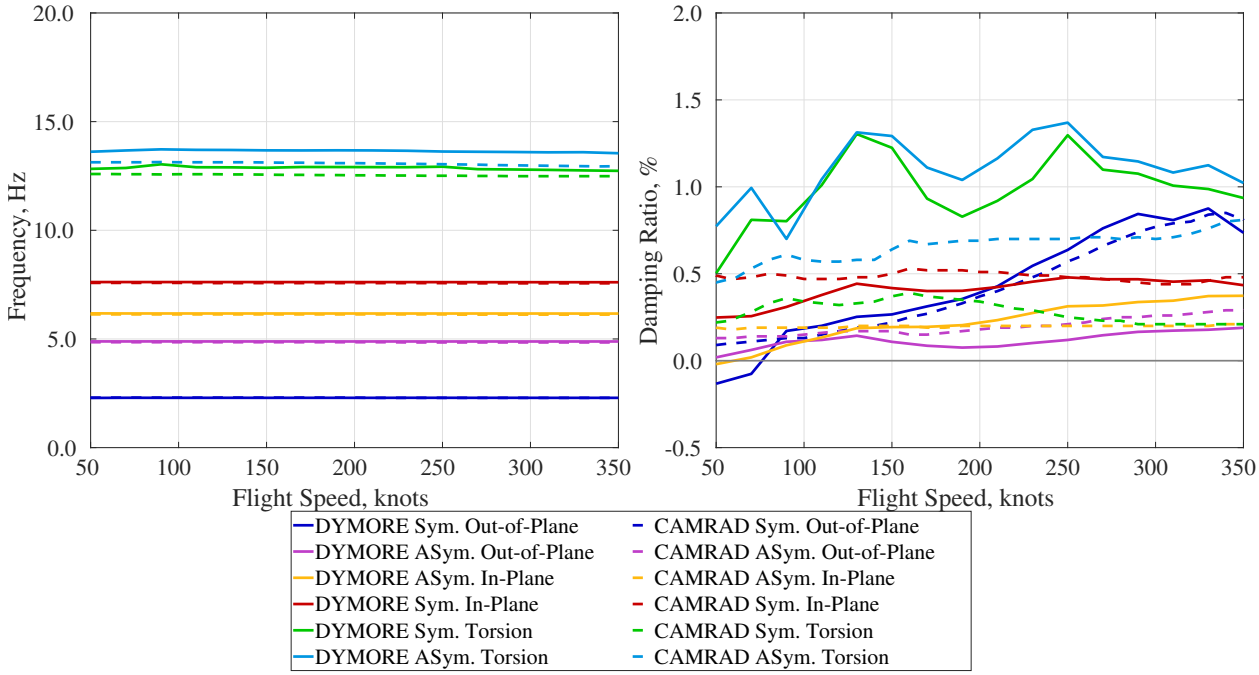

Fig. 9 Wing Frequency and Damping Ratio vs. Flight Speed, Schedule High-Lift Propeller RPM.

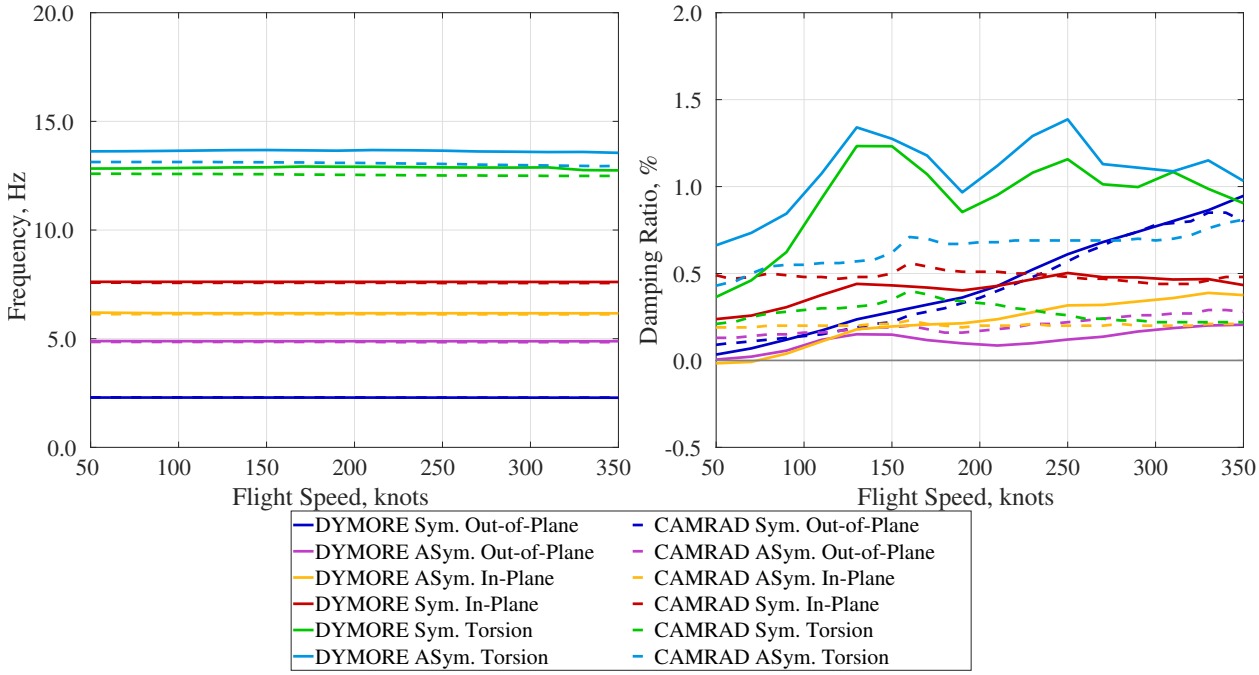

Fig. 10 Wing Frequency and Damping Ratio vs. Flight Speed, Overspeed High-Lift Propeller 5940 RPM.

generally higher damping ratios for the two torsion modes than those by CAMRAD, again due to the difference in tip propeller blade models.

IV. Summary and Conclusion

Multibody dynamics codes, Dymore and CAMRAD, are used to model and predict the propeller whirl-flutter stability of the NASA X-57 Maxwell with all 14 propellers. A modal super-element (MSE) is used to capture the structural dynamics of the X-57 full-span wing, fuselage, and tail section for the Dymore model. The MSE is derived from the full degree of freedom NASTRAN FEM model with a component mode synthesis approach (Herting reduction).

The Dymore model is used to perform a parametric study of high-lift propeller location along the leading edge of the wing on whirl-flutter stability. The damping ratios of wing modes are generally low because of the small sizes of those high-lift propellers. The most outboard pair of high-lift propellers has the highest damping ratio for the first symmetric wing out-of-plane bending mode and torsion mode. The high-lift propeller location influence on the first symmetric wing inplane mode is mixed. The variation of damping ratio vs speed shows different trends depending on the locations of the high-lift propeller pairs. The damping of antisymmetric out of plane and inplane modes are only slightly affected by the locations of the high-lift propellers.

Both Dymore and CAMRAD models are used to predict the whirl-flutter stability of the X-57 with all 14 propellers. The cruise flight RPM 2700 is selected for the tip propeller while three high-lift propeller RPM are selected: 0 (simulating high-lift propeller folded to nacelle), a scheduled RPM variation with speed, an overspeed case at 5940. Agreement between Dymore and CAMRAD is good for the first four modal frequencies studied for all three high-lift propeller RPM cases. Overall good agreement is also observed between the two codes for the predictions of the damping ratio variations of wing modes with speed except for torsional modes. The torsional modes show some discrepancies due to different blade structure models used in the two codes. Dymore predicts the torsional mode damping twice as great as that calculated by CAMRAD. This is because Dymore models tip-propeller blade flexibility, while CAMRAD does not. The results show no indication of propeller whirl flutter with the exception of the very small negative damping at low flight speeds predicted by Dymore at a few cases. The component mode synthesis element demonstrates its capability to model systems with complex structural dynamics, such as the X-57 with its multiple propeller interface nodes, as well as its ability to predict multipropeller whirl-flutter stability boundaries when implemented in a multibody dynamics analysis.

V. Acknowledgements

The first two authors were funded by the NASA Langley Research Center (LaRC) through the National Institute of Aerospace with Jefffrey Viken as the technical monitor. The authors would like to thank Keerti Bhamidipati (NASA Armstrong Research Center) and David Piatak (LaRC) for their support of this study. The Dymore analysis is kindly provided by Olivier Bauchau at University of Maryland, College Park (UMD). We also knowledge the help from Matteo Scapolan (UMD) on the Dymore modal-super-element.

References

[1] Heeg, J., and Stanford, B. K., "Whirl Flutter and the Development of the NASA X-57 Maxwell," *International Forum on Aeroelasticity and Structural Dynamics*, Hampton, VA, 2019.

[2] Viken, J. K., Viken, S., Deere, K. A., and Carter, M., "Design of the Cruise and Flap Airfoil for the X-57 Maxwell Distributed Electric Propulsion Aircraft," *35th AIAA Applied Aerodynamics Conference*, 2017, p. 3922.

[3] Deere, K. A., Viken, J. K., Viken, S., Carter, M. B., Wiese, M., and Farr, N., "Computational analysis of a wing designed for the X-57 distributed electric propulsion aircraft," *35th AIAA applied aerodynamics conference*, 2017, p. 3923.

[4] Murray, J., and Lechniak, J., "The LEAPTech Experiment, Approach, Results, Recommendations," Tech. rep., 2016.

[5] Patterson, M. D., and Borer, N. K., "Approach considerations in aircraft with high-lift propeller systems," *17th AIAA Aviation Technology, Integration, and Operations Conference*, 2017, p. 3782.

[6] Taylor, E. S., and Browne, K. A., "Vibration Isolation of Aircraft Power Plants," 1938.

[7] Reed, W. H., "Propeller-rotor whirl flutter: A state-of-the-art review," 1966, pp. 526–544. doi:https://doi.org/10.1016/0022-460X(66)90142-8.

[8] Abbott, F. T., Kelly, H., and Hampton, K. D., "Investigation of Propeller-Power-Plant Autoprecession Boundaries for a Dynamic-Aeroelastic Model of a Four-Engine Transport Airplane," 1963.

[9] Cecrdle, J., *Whirl flutter of turboprop aircraft structures*, Woodhead Publishing, 2015.

[10] Shen, J., and Kang, H., "Comparison Study of Tiltrotor Whirl Flutter Using Two Rotorcraft Comprehensive Analyses," *Journal of Aircraft*, Vol. 54, No. 2, 2017, pp. 845–850. doi:10.2514/1.C033905.

[11] Kang, H., Shen, J., and Kreshock, A., "Validation of Comprehensive Analysis for Tiltrotor Whirl Flutter Predictions," *Joural of Aircraft*, Vol. 54, No. 4, 2017, pp. 1566–1570.

[12] Yeo, H., Bosworth, J., Acree Jr, C., and Kreshock, A. R., "Comparison of CAMRAD II and RCAS predictions of tiltrotor aeroelastic stability," *Journal of the American Helicopter Society*, Vol. 63, No. 2, 2018, pp. 1–13.

[13] Kreshock, A., Acree, H., Cecil snf Kang, and Teo, H., "Development of a new aeroelastic tiltrotor wing tunnel testbed," *AIAA SciTech 2019 Forum*, 2019, p. 2133.

[14] Yeo, H., and Kreshock, A. R., "Whirl flutter investigation of hingeless proprotors," *Journal of Aircraft*, Vol. 57, No. 4, 2020, pp. 586–596.

[15] Koutsovasilis, P., and Beitelschmidt, M., "Comparison of model reduction techniques for large mechanical systems," *Multibody System Dynamics*, Vol. 20, No. 2, 2008, pp. 111–128.

[16] Besselink, B., Tabak, U., Lutowska, A., Van de Wouw, N., Nijmeijer, H., Rixen, D. J., Hochstenbach, M., and Schilders, W., "A comparison of model reduction techniques from structural dynamics, numerical mathematics and systems and control," *Journal of Sound and Vibration*, Vol. 332, No. 19, 2013, pp. 4403–4422.

[17] Sonneville, V., Scapolan, M., Shan, M., and Bauchau, O. A., "Modal reduction procedures for flexible multibody dynamics," *Multibody System Dynamics*, Vol. 51, No. 4, 2021, pp. 377–418.

[18] Bauchau, O., Bottasso, C., and Nikishkov, Y., "Modeling Rotorcraft Dynamics with Finite Element Multibody Procedures," *Mathematical and Computer Modeling*, Vol. 33, 2001, pp. 1113–1137.

[19] Johnson, W., "Technology Drivers in the Development of CAMRAD II," *American Helicopter Society Aeromechanics Specialists Conference*, San Francisco, CA, 1994.

[20] Hoover, C. B., "Propeller Whirl Flutter Analysis of the NASA All-Electric X-57 Through Multibody Dynamics Simulation," 2018.

[21] Bauchau, O. A., *Dymore Users Manual*, 2016.

[22] Weiss, L., and McDonough, R. N., "Prony's Method, Z-Transforms, and Padé Approximation," *SIAM Review*, Vol. 5, No. 2, 1963, pp. 145–149. doi:10.1137/1005035.

[23] Nelson, K., Shen, J., Scapolan, M., and Bauchau, O., "Propeller Whirl Flutter Study using Multibody Dynamics Analysis with Component Mode Synthesis Element," *AIAA SCITECH 2022 Forum*, San Diego, CA, 2022, p. 1125.